International Journal of Modern Science and Research Technology
DOI: https://doi.org/10.67317/IJMSRT26AUG166

Assessment of Borehole Failure in the Global South: Integrated Hydrogeological and Geophysical Evidence from Gombe Metropolis, Northeastern Nigeria

*Amos Ibrahim S; Adewoyin J.E; Ozuem C.D; Aigbiremolen I.M
Oyetoro G.G; Oladiran O.E; Idris I.A

National Space Research and Development Agency, Cooperative Information Network, Obafemi Awolowo University, Ile-Ife, South-West Nigeria

***Corresponding author**

Abstract

Groundwater underpins domestic water supply across much of the Global South, yet chronic borehole failure continues to undermine investment in water-supply infrastructure, particularly in geologically heterogeneous sedimentary basins where site selection is rarely constrained by integrated subsurface data. This study presents an integrated hydrogeological, geophysical, and statistical assessment of groundwater occurrence and borehole performance in Gombe Metropolis, northeastern Nigeria, a rapidly urbanizing city of approximately 450,000 people situated within the Gongola Sub-basin of the Upper Benue Trough. A compiled inventory of 71 borehole records (depth, functional status, and, where available, yield) was cross-referenced against 23 Vertical Electrical Sounding (VES) stations acquired using the Schlumberger configuration, in order to constrain otherwise non-unique geoelectric interpretation with authentic subsurface ground-truth. Complete depth and functional-status data were available for 58 of the 71 boreholes (35 functioning, 23 not functioning), forming the basis for formal statistical testing, while a richly documented subset of 32 boreholes (24 with individually reported depths) supported a ward-level qualitative analysis of failure mechanisms. Non-functional boreholes cluster in the wards of Bolari and Jakada Fari at shallow-to-intermediate depths, where thick sequences of the Pindiga (Fika) Shale, ironstone intercalations within the middle member of the Gombe Formation, and structurally attenuated stratigraphy act as hydrogeological barriers; however, a Mann–Whitney U test across the full 58-record subset found that borehole depth alone did not significantly distinguish functioning (mean 86.6 ± 29.3 m) from non-functioning boreholes (mean 72.0 ± 31.0 m; U = 505.0, $p = 0.105$, rank-biserial r = 0.255). Across the 23 VES stations, groundwater potential was descriptively associated with aquifer lithology (Cramér's V = 0.423) though this did not reach significance in a Fisher–Freeman–Halton exact test ($p = 0.458$) given the small, sparse sample; clean, fine-grained sand and sandstone units nonetheless hosted the majority of high-potential occurrences, whereas silty and clay-dominated facies were predominantly moderate to poor except where deeply confined (> 135 m). In contrast, aquiferous depth was strongly and significantly correlated with VES-derived groundwater-potential class (Spearman $\rho = 0.682$, $p < 0.001$; Kruskal–Wallis H (2) = 12.63, $p = 0.002$). A shallow functional outlier and a fault-associated deep success zone near Pantami confirm that depth alone is an incomplete predictor of borehole outcome. Taken together, the statistical and geological evidence indicates that borehole failure in Gombe Metropolis is governed jointly by aquiferous depth and lithological confinement rather than by depth in isolation, and that borehole ground-truthing is indispensable for resolving the inherent ambiguity of VES interpretation in structurally complex sedimentary terrains. The findings provide an evidence-based basis for depth-targeted drilling, ward-specific development planning, and groundwater protection policy in Gombe and analogous basins across the Global South.

Keywords: Groundwater Potential; Borehole Failure; Vertical Electrical Sounding; Upper Benue Trough; Gombe Formation; Global South; Aquifer Ground-Truthing; Non-Parametric Statistics.

1. Introduction

Groundwater constitutes the largest accessible reserve of freshwater on Earth and plays a fundamental role in sustaining domestic water supply, food production, industrial development, ecosystem functioning, and climate resilience worldwide (Coomar et al.,2020). In recent decades, groundwater has become increasingly important for global water security in the face of growing pressure on surface-water resources from population growth, urbanization, land-use change, and climate variability (Cuthbert, M. 2026). Unlike many surface-water systems, groundwater often provides a comparatively reliable and drought-resilient source of freshwater, particularly in semi-arid and arid environments where rainfall is highly seasonal (Cuthbert et al., 2019; Ascott et al., 2022), and its development is increasingly recognized as central to climate adaptation and to Sustainable Development Goal 6 (universal access to safe and affordable drinking water).

Sub-Saharan Africa (SSA), a region broadly representative of the wider Global South in its groundwater dependence and infrastructure constraints, is among the most reliant on this resource. The majority of rural populations, and a growing share of urban populations, depend on groundwater for drinking water, sanitation, agriculture, and small-scale economic activity (Braune & Xu, 2010; Xu et al., 2019). MacDonald et al. (2012) demonstrated that groundwater storage across Africa is considerably larger than previously assumed and may exceed annual renewable freshwater resources by more than two orders of magnitude; nonetheless, the spatial distribution of productive aquifers is highly heterogeneous, ranging from extensive sedimentary basins to fractured crystalline basement terrains, and groundwater resources across the region remain relatively underdeveloped relative to their estimated potential (Cuthbert, et al., 2019; Cobbing & Hiller, 2019).

Despite this promise, access to sustainable groundwater supplies remains constrained by technical, hydrogeological, institutional, and management challenges. One of the most persistent is the high incidence of borehole failure, particularly in low- and middle-income countries, where exploration and development often proceed under limited hydrogeological information and inadequate technical supervision (Danert et al., 2020; Danert et al., 2022). Failure may take the form of low or seasonally variable yield, poor water quality, mechanical breakdown, casing collapse, or premature abandonment shortly after construction, and it represents a substantial economic loss that undermines confidence in water-supply investment, particularly where alternative sources are limited (Danert et al., 2020).

Prior work attributes borehole failure principally to poor site selection, inadequate hydrogeophysical investigation, incomplete understanding of aquifer characteristics, inappropriate drilling method, and weak post-construction management (Foster & MacDonald, 2014; Danert et al., 2022). In basement complex terrains, groundwater occurrence is governed largely by weathered regolith thickness, fracture density, and structural connectivity, whereas in sedimentary environments productivity is instead controlled by porosity, permeability, depositional facies, and structural deformation (Hansani et al., 2025). Consequently, successful groundwater development increasingly depends on integrating geological, hydrogeological, geophysical, and geospatial evidence to delineate productive aquifer zones and reduce drilling risk. Recent advances, including geographic information systems, remote sensing, multi-criteria decision analysis, and machine learning, have improved groundwater-potential mapping and borehole siting in data-scarce environments (Saidu et al., 2024; Jimoh et al., 2025; Babaye et al., 2021), yet the integration of borehole ground-truth with geophysical survey remains the most direct means of resolving the non-uniqueness inherent in geoelectric inversion.

Nigeria is among the largest groundwater-dependent countries in Africa, its dependence intensified by rapid population growth, urbanization, recurrent drought, and inadequate public water-supply infrastructure (Egbueri, et al., 2025). Groundwater occurrence spans sedimentary basins, crystalline basement terrains, volcanic formations, and alluvial deposits, each with distinct hydrogeological behaviour (Adelana & MacDonald, 2008), and borehole productivity therefore varies considerably across the country. Investigations in the Middle Benue Trough attribute widespread low-yielding and failed boreholes to poor aquifer transmissivity and hydraulic conductivity; studies in southwestern Nigeria link low productivity to shallow weathered layers, poor fracture development, and inadequate exploration depth (Obi et al., 2026; Olabanji et al., 2024); and basement-terrain geophysical surveys confirm that productive zones are often localized and difficult to identify without detailed subsurface characterization (Raji & Abdulkadir, 2020; Osinowo & Arowoogun, 2020). Collectively, these findings underline the necessity of integrating hydrogeological and geophysical investigation into groundwater development projects.

This challenge is particularly acute in northeastern Nigeria, where climatic variability, recurrent drought, and population growth intensify pressure on groundwater resources. Gombe State lies within the Upper Benue Trough and adjoining basement-influenced terrain, where groundwater occurrence is controlled by a complex interaction of lithology, weathering, structural deformation, fracturing, and sedimentary architecture. Sandstone units, notably the Gombe Sandstone and related formations, possess relatively favorable aquifer properties, but groundwater occurrence remains highly localized and structurally controlled (Saidu et al., 2025). Despite groundwater being the primary source of potable water for many communities in the state, comprehensive assessments linking borehole failure patterns to groundwater potential remain scarce; existing studies have concentrated on groundwater occurrence, hydro geochemistry, or localized geophysical survey, with limited attention to the spatial relationship between borehole performance and groundwater potential. This gap constrains evidence-based groundwater development and risks perpetuating investment in unsuccessful boreholes.

Addressing this gap matters beyond Gombe. The city is an instructive case of a broader Global South condition: rapid urban growth outpacing planned water infrastructure, historic drilling records that are rarely centralized or digitized, and geophysical survey that is seldom rigorously constrained by borehole ground-truth before being acted upon. The present study responds directly to this condition by assessing borehole failure and groundwater potential in Gombe Metropolis through an integrated evaluation of geological, hydrogeological, geophysical, borehole-performance, and statistical evidence. Specifically, the study aims to: (i) characterize the stratigraphic and structural controls on aquifer distribution in Gombe Metropolis; (ii) compile and analyze the operational status of a substantial borehole inventory to identify the depth ranges and wards most associated with failure; (iii) interpret Vertical Electrical Sounding data across the metropolis and classify groundwater potential by inferred aquifer lithology; (iv) statistically test the strength of the depth–functionality and lithology–potential relationships rather than relying on descriptive pattern alone; and (v) constrain the geoelectric interpretation against authentic borehole logs to resolve cases of non-unique or misleading resistivity signatures, translating the combined findings into evidence-based recommendations for depth-targeted drilling, ward-specific planning, and groundwater protection.

The study contributes to the literature in three respects. First, it presents one of the more extensive boreholes–VES ground-truthing exercises reported for the Upper Benue Trough, explicitly using borehole records, and formal non-parametric statistical testing, to adjudicate ambiguous geoelectric signatures rather than treating VES interpretation as self-sufficient. Second, it demonstrates, with ward-level specificity, how a single depositional and structural setting — the Gombe Formation and its bounding fault — can simultaneously produce a shallow failure zone and a deep, fault-associated success zone within a few kilometres of one another. Third, it provides a transparent account of the limits of the underlying dataset, so that the conclusions drawn are calibrated to the evidence actually available rather than overstated. The remainder of this paper is organized as follows: Section 2 describes the study area and its geological and tectonic framework; Section 3 details the materials and methods, including the statistical approach; Section 4 presents the results; Section 5 discusses their hydrogeological and practical implications; and Section 6 concludes with recommendations for groundwater development and management.

2. Study Area

2.1 Location, Climate, and Water Demand

Gombe Metropolis is the capital of Gombe State, northeastern Nigeria, and lies within the Gongola Sub-basin of the Upper Benue Trough. The metropolis has undergone rapid urbanization over the past two decades and now supports a population approaching 450,000. Public and private water supply remains intermittent, producing an acute disparity between estimated per capita demand of 108.7 litres per day and actual delivered supply, a gap that groundwater abstraction, largely through private and community boreholes, has come to fill by default rather than by design.

ISSN:2584-2706 DOI: https://doi.org/10.67317/IJMSRT26AUG166

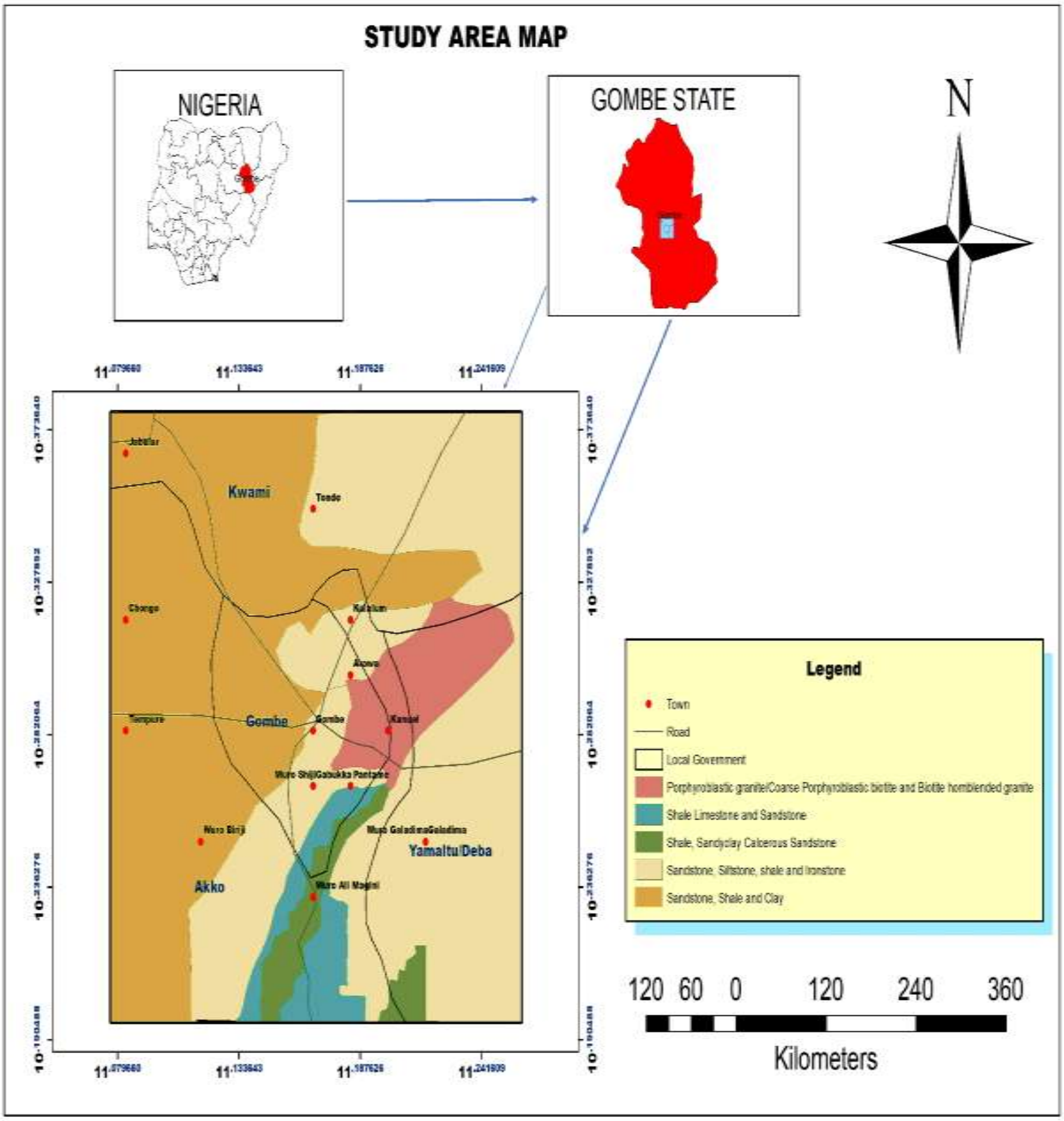

Figure 1. Location and geological setting of the study area

2.2 Regional Stratigraphy and Depositional Environments

The hydrogeology of Gombe is rooted in its position within the Upper Benue Trough, a major rift structure formed during the Cretaceous period. The stratigraphic succession in the metropolis comprises, from oldest to youngest, the Precambrian Basement Complex, the Bima Sandstone, the Yolde Formation, the Pindiga Formation, and the Gombe Formation, locally capped by the Tertiary Kerri-Kerri Formation and Quaternary Alluvium (Figure 2; Table 1).

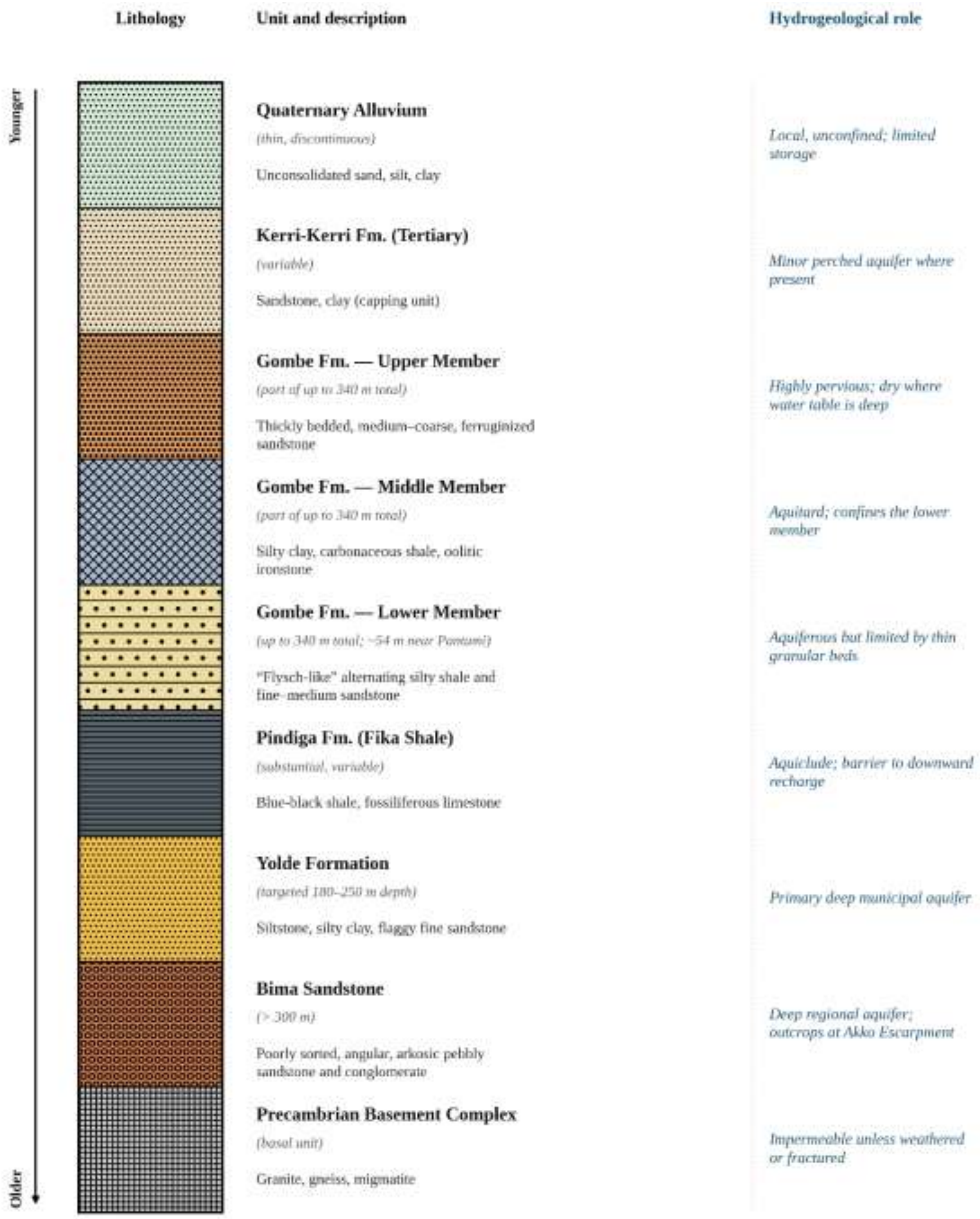

Figure 2. Schematic stratigraphic succession of the Gombe Metropolis area and inferred hydrogeological role of each unit (not to scale)

Table 1. Stratigraphic succession of the Gombe Metropolis area and inferred hydrogeological role

Unit (youngest to oldest)	Approx. thickness	Lithology	Hydrogeological role
Quaternary Alluvium	Thin, discontinuous	Unconsolidated sand, silt, clay	Local, unconfined; limited storage
Kerri-Kerri Fm. (Tertiary)	Variable	Sandstone, clay (capping unit)	Minor perched aquifer where present

Gombe Fm. — Upper Member	Part of up to 340 m total	Thickly bedded, medium–coarse, ferruginized sandstone	Highly pervious; dry where water table is deep
Gombe Fm. — Middle Member	Part of up to 340 m total	Silty clay, carbonaceous shale, oolitic ironstone	Aquitard; confines the lower member
Gombe Fm. — Lower Member	Part of up to 340 m total; attenuated to ~54 m near Pantami	"Flysch-like" alternating silty shale and fine–medium sandstone	Aquiferous but limited by thin granular beds
Pindiga Fm. (Fika Shale)	Substantial, variable	Blue-black shale, fossiliferous limestone	Aquiclude; barrier to downward recharge
Yolde Formation	Targeted 180–250 m depth	Siltstone, silty clay, flaggy fine sandstone	Primary deep municipal aquifer
Bima Sandstone	> 300 m	Poorly sorted, angular, arkosic pebbly sandstone and conglomerate	Deep regional aquifer; outcrops at Akko Escarpment
Precambrian Basement Complex	Basal unit	Granite, gneiss, migmatite	Impermeable unless weathered or fractured

2.3 Tectonic Control: The Gombe Fault

The Gombe Fault is a major structural feature trending north-south through the metropolis. It has significantly influenced sedimentation patterns and the present spatial distribution of rock units, and near Pantami it brings the Lower Gombe Sandstone into vertical contact with the Bima Group, creating structural boundaries that either compartmentalize or channel groundwater flow. Tectonism has also attenuated certain formations; the Gombe Formation, for example, thins to approximately 54 m near Kwanan Pantami, directly reducing the storage capacity of the local aquifer (Table 1).

3. Materials and Methods

3.1 Research Design

The study adopts a correlational, data-driven design intended to identify systematic relationships between reservoir and structural properties of the subsurface (independent variables) and observed borehole outcome (dependent variable), constrained throughout by authentic in-situ borehole records and tested with appropriate non-parametric statistical methods. The approach follows the principle that geophysical models are inherently non-unique and that borehole information provides the most reliable empirical benchmark against which resistivity-based interpretation must be calibrated.

3.2 Borehole Inventory and Functionality Assessment

A dataset of 71 borehole points across Gombe Metropolis was compiled from Gombe State Rural Water Supply and Sanitation Agency (RUWASSA) records and a field verification survey between December 15 2025 to February 15 2026. For each borehole, location (ward/community), total depth, and current operational status were recorded, together with static water level and discharge (yield) where available. Boreholes were classified as functional where they sustained a discharge of at least 0.5 L/s at the time of survey, and non-functional where they were dry, yielded below this threshold, or had been abandoned; this operational definition follows conventions applied in prior regional borehole-failure assessments (Danert et al., 2020; Danert et al., 2022). The 71-record inventory supported analysis at three levels of completeness: complete depth and functional-status values were available for 58 records (35 functioning, 23 not functioning), which formed the basis of the formal statistical comparison in Section 3.5 and Section 4.6; a richly documented subset of 32 boreholes, for which ward, depth, status, and the corresponding nearest VES station are individually itemized, is reported in full in Table 2 and underpins the ward-level qualitative analysis in Sections 4.1, 4.3, and 4.4; and of these, 24 boreholes had individually reported depth values suitable for the documented depth-status pattern illustrated in Section 4.6. The complete 71-record inventory, including coordinates, is available reasonable request from the corresponding Author.

3.3 Geophysical (VES) Data Acquisition

Twenty-three Vertical Electrical Sounding (VES) stations were acquired across the metropolis using the Schlumberger electrode configuration, with a maximum current electrode spacing (AB/2) of 300m to achieve adequate depth of investigation for the deep aquifer targets identified in Section 2. Field measurements were acquired using ABEM Terameter LS over the survey period. Apparent resistivity data were processed and inverted using an inversion software (IPI2Win) to derive layer resistivity, thickness, and depth, following standard partial curve-matching and computer-assisted inversion procedures. Resulting curve types were classified according to conventional nomenclature (H, A, K, Q and their combinations), and resistivity ranges were assigned lithological identities based on the comparative ranges in Table 3, informed by known regional lithology.

3.4 Ground-Truthing: Constraining VES with Borehole Logs

Each VES station was spatially paired with the nearest borehole record(s) for which depth and functional status were known, allowing the inferred geoelectric layering to be checked directly against observed drilling outcome. Where a high-resistivity layer could plausibly represent either dry sand, ironstone, or compacted bedrock, the corresponding borehole log was used to resolve the ambiguity. This ground-truthing step, combined with the formal statistical testing described below, is the central methodological contribution of the study and is applied systematically in Section 4.

3.5 Statistical and Analytical Methods

Three analytical relationships were tested statistically, in addition to the qualitative ward-level ground-truthing described above: (i) the association between inferred aquifer lithology and groundwater-potential class; (ii) the relationship between borehole depth and functional status; and (iii) the relationship between aquiferous depth and groundwater-potential class.
For the VES dataset, reported aquiferous-depth ranges were converted to representative midpoint values using Equation 1,

$$D_m = \frac{D_{lower} + D_{upper}}{2}$$

where D_m is the aquiferous-depth midpoint and D_lower and D_upper are the lower and upper reported depth boundaries, respectively. For example, an interpreted aquiferous interval of 150–160 m was represented by a midpoint of 155 m. Groundwater potential was treated as an ordered categorical variable with three classes (Poor, Moderate, High), coded ordinally as 1, 2, and 3 for rank-based analyses; this coding did not imply that successive classes were equally spaced.
The association between inferred aquifer lithology and groundwater-potential class was examined using a contingency table and frequency distribution, visualized as a stacked bar chart (Figure 3). Because both variables were categorical, the VES sample comprised only 23 interpreted locations, and the resulting contingency table contained sparse cells with small expected frequencies, the primary inferential analysis used the Fisher–Freeman–Halton exact test, which extends Fisher's exact test to contingency tables larger than 2 × 2 and is appropriate where expected cell frequencies are small. Pearson's chi-square statistic was also calculated as a supplementary descriptive measure, but because the assumptions underlying the asymptotic chi-square approximation were not fully satisfied, the exact test was treated as the principal significance test. The magnitude of association was quantified using Cramér's V (Equation 2),

$$V = \sqrt{\frac{\chi^2}{N \times \min(r-1, c-1)}}$$

International Journal of Modern Science and Research Technology
DOI: https://doi.org/10.67317/IJMSRT26AUG166

where χ^2 is the Pearson chi-square statistic, N is the total number of observations, and r and c are the number of rows and columns in the contingency table. Cramér's V was interpreted as an effect-size measure rather than a test of statistical significance. Statistical significance throughout was evaluated at $\alpha = 0.05$.

The relationship between borehole depth and functional status was investigated using descriptive statistics (mean, standard deviation, median, minimum, maximum) for the 58 boreholes with complete depth and status data, summarized in a depth-by-status box plot (Figure 5). A Mann–Whitney U test was used to compare depths between functioning and non-functioning groups; this non-parametric test was preferred to the independent-samples t-test because depth distributions were not assumed to satisfy normality and equal-variance assumptions. A rank-biserial correlation was additionally calculated to quantify the magnitude and direction of the difference, since a p-value alone does not indicate practical effect size.

The relationship between interpreted aquiferous depth and groundwater potential was examined using the midpoint of each reported VES aquiferous-depth interval (Figure 6). Spearman's rank-order correlation (ρ) was used to quantify the monotonic relationship between aquiferous depth and the ordinal groundwater-potential score. A Kruskal–Wallis H test was additionally performed on aquiferous-depth midpoints to provide an independent, non-parametric comparison among the three groundwater-potential classes.

Analyses were conducted in Python (pandas, NumPy, SciPy, and matplotlib), with Microsoft Excel used for preliminary data organization and categorical validation. The principal categorical and non-parametric analyses were additionally structured for independent verification in IBM SPSS Statistics: the lithology–potential analysis was verified using the Crosstabs procedure with chi-square and measures of association (Exact Tests option applied for the sparse contingency table); the borehole-depth comparison was verified using the independent-samples Mann–Whitney U procedure; and Spearman's rank correlation and the Kruskal–Wallis procedure provided independent verification of the depth–potential analyses.

3.6 Data Limitations

In the interest of scientific transparency, the following limitations of the underlying dataset are stated explicitly. First, individually attributable ward, depth, status, and nearest-VES data are available for 32 of the 71 compiled boreholes (24 with depth values suitable for the documented depth-status illustration in Section 4.6); complete depth and functional-status values (without full ward-level itemization) are available for 58 of the 71 records and were used for the formal Mann–Whitney comparison. The remaining records exist in the source inventory but are not individually itemized in this paper and should be included in Supplementary Table S1 prior to submission. Second, VES station coordinates are not yet tabulated; a coordinate table and GIS map (Figure 1) should be finalized before submission, as spatial claims in a hydrogeology paper require verifiable station locations. Third, several methodological details — electrode spacing, survey dates, field instrumentation, and inversion software — are flagged in Sections 3.2–3.3 for author confirmation from the original field records rather than assumed.

4. Results

4.1 Documented Borehole Inventory

Table 2 presents the 32 boreholes for which ward, depth and functional status are individually documented in the compiled inventory (of 71 total records; complete depth and status values were available for 58 records overall, forming the basis of the formal statistical test in Section 4.6). The pattern confirms that depth alone does not guarantee a functional well: BH46 in Kumbiya-Kumbiya was drilled to 120 m but remains non-functional, whereas BH39 in Mai Angwa Kwaranga is functional at a shallow depth of only 36 m. Wards such as Shamaki and Herwagana show a higher concentration of functional wells, with reported yields in Shamaki ranging between 0.5 and 10.0 L/s, whereas Bolari and Jakada Fari are dominated by non-functional points, including wells reaching 78 m depth without producing water.

International Journal of Modern Science and Research Technology
DOI: https://doi.org/10.67317/IJMSRT26AUG166

Table 2. Documented borehole inventory referenced in this study (n = 32 of 71).

Ward / Community	BH Code	Depth (m)	Status	Yield (L/s)	Corresponding VES
Bolari West	B1	48	Non-functional	0.35	VES 9 (Doma Plaza)
Bolari West	B2	30	Non-functional	0.40	VES 9 (Doma Plaza)
Bolari East	B3	45	Non-functional	0.1	VES 4 (Dubai Qtrs)
Bolari East	B9	54	Non-functional	0.3	VES 4 (Dubai Qtrs)
Bolari East	B14	54	Non-functional	0.0	VES 4 (Dubai Qtrs)
Jakada Fari	B4	78	Non-functional	0.1	VES 10 (Opp. Govt House)
Jakada Fari	B10	54	Non-functional	0.2	VES 10 (Opp. Govt House)
Jakada Fari	B11	78	Non-functional	0.0	VES 10 (Opp. Govt House)
Jakada Fari	B19	90	Non-functional	0.12	VES 10 (Opp. Govt House)
Dawaki (North)	B52	108	Non-functional	0.1	VES 14 (Dawaki Qtrs)
Dawaki (North)	B61	78	Non-functional	0.0	VES 14 (Dawaki Qtrs)
Dawaki (North)	B64	78	Non-functional	0.0	VES 14 (Dawaki Qtrs)
Kumbiya-Kumbiya	B46	120	Non-functional	0.0	VES 12 (New GRA)
Shamaki (failed sites)	B30	58	Non-functional	0.0	VES 3 / VES 11
Shamaki (failed sites)	B32	108	Non-functional	0.0	VES 3 / VES 11
Shamaki (failed sites)	B37	86	Non-functional	0.3	VES 3 / VES 11
Shamaki (failed sites)	B42	96	Non-functional	1.0-4.0	VES 3 / VES 11
Shamaki (failed sites)	B43	84	Non-functional	0.2	VES 3 / VES 11
Shamaki (failed sites)	B70	50	Non-functional	0.4	VES 3 / VES 11
Pantami (shallow)	B21	27	Non-functional	0	—

ISSN:2584-2706 DOI: https://doi.org/10.67317/IJMSRT26AUG166

Ward / Community	BH Code	Depth (m)	Status	Yield (L/s)	Corresponding VES
Mai Angwa Kwaranga	B39	36	Functional	11.0	—
Shamaki	B40	128	Functional	10.0	VES 16 (Kagarawal)
Shamaki	B13	125	Functional	0.5–10.0 (ward range)	VES 16 (Kagarawal)
Shamaki	B34	120	Functional	0.5–10.0 (ward range)	VES 16 (Kagarawal)
Shamaki	B47	100	Functional	0.5–10.0 (ward range)	VES 16 (Kagarawal)
Herwagana	B53	90	Functional	0.8-9.0	VES 8 (Kanoyel Qtrs)
Herwagana	B56	110	Functional	10.0	VES 8 (Kanoyel Qtrs)
Herwagana	B66	90	Functional	0.5-9.0	VES 8 (Kanoyel Qtrs)
Dawaki (Central)	B51	95	Functional	0.7-10.0	—
Dawaki (Central)	B59	100	Functional	0.9-11.0	—
Dawaki (Central)	B60	110	Functional	11.0 above	—
Pantami (deep)	B15	~95 (range 90–100)	Functional	10.0-15.0	—

4.2 Resistivity Signatures of Lithological Units

Interpretation of VES curves across Gombe requires differentiating the high-resistivity signatures of laterite, ironstone, and dry sandstone from the low-resistivity signatures of clay, shale, and water-bearing sand. Table 3 summarizes the resistivity ranges assigned to each lithological class and their hydrogeological significance.

Table 3. Comparative resistivity ranges for lithological identification.

Lithology	Typical resistivity range (Ωm)	Hydrogeological significance
Topsoil / laterite	66 – 2,033	Protective overburden; resistivity varies with moisture content

ISSN:2584-2706 DOI: https://doi.org/10.67317/IJMSRT26AUG166

Lithology	Typical resistivity range (Ωm)	Hydrogeological significance
Dry sandstone	250 – 900	High primary porosity but lacks saturation
Saturated sandstone	100 – 600	Optimal aquifer target; yield depends on grain sorting
Sandy clay	28 – 84	Moderate groundwater potential; prone to low yield
Shale (Fika / Pindiga)	3 – 57	Aquiclude; barrier to downward groundwater recharge
Ironstone / compact layers	2,069 – 17,456	Impermeable; acts as an aquitard or basement mimic

The shape of the VES curve provides a qualitative indication of subsurface layering. The H-type curve ($\rho_1 > \rho_2 < \rho_3$), representing a conducting middle layer between two resistive layers, is the most sought-after signature for borehole siting in Gombe. The HK-type indicates a four-layer sequence in which a productive conductive zone is succeeded by a resistive layer, typically ironstone or compacted sandstone. The A-type, a steady increase in resistivity with depth, suggests a thin topsoil over a massive, compact formation with no major aquifer. The QH-type, encountered in fractured shale terrains, shows a progressively more conductive sequence culminating in a fractured, water-bearing horizon.

4.3 VES Points and Borehole Correlation in Unproductive Areas

Table 4 presents the correspondence between non-functional borehole clusters and the nearest VES station, together with the inferred lithological barrier responsible for failure.

Table 4. Borehole points and corresponding VES stations in water-stressed (unproductive) areas.

Ward / Community	BH points	Depth range (m)	Corresponding VES	Primary geological / lithological barrier
Bolari West	B1, B2	15 – 110 (ward-scale VES depth)	VES 9 (Doma Plaza)	Dominant sequence of bluish-greenish dry shale (Pindiga Fm.)
Bolari East	B3, B9, B14	10 – 54	VES 4 (Dubai Qtrs)	Ironstone intercalations and thin sand layers over thick dry shale
Jakada Fari	B4, B10, B11, B19	54 – 91	VES 10 (Opp. Govt House)	Ironstone and mudstone sequence to 91 m; “flysch-like” non-aquiferous sedimentation
Dawaki (North)	B52, B61, B64	78 – 108	VES 14 (Dawaki Qtrs)	Pale gypsiferous shale and thick dry

ISSN:2584-2706 DOI: https://doi.org/10.67317/IJMSRT26AUG166

				shale barriers (up to 70.5 m)
Kumbiya-Kumbiya	B46	120	VES 12 (New GRA)	Deep compacted sand, ironstone and mudstone mimicking bedrock
Shamaki (failed sites)	B30, B32, B37, B42, B43, B70	50 – 108	VES 3 / VES 11	Aquitards (middle Gombe member) and low-yield silty shale
Pantami (shallow)	B21	27	—	Insufficient depth to bypass the Upper Gombe Sandstone

At Doma Plaza (VES 9), the geoelectric sequence is dominated by 96.9 m of bluish-greenish dry shale; boreholes B1 and B2, terminating at 48 m and 30 m respectively, were therefore drilled entirely within this impermeable unit. Similarly, at Jakada Fari, VES 10 identifies ironstone and mudstone to a depth of 91 m, consistent with the failure of B10 (54 m) and B11 (78 m).

4.4 Functional Borehole Points and Corresponding VES in Productive Areas

In contrast, Shamaki and Herwagana display a higher density of successful water points, corresponding to granular sandstone units identified geoelectrically at 55–110 m depth, often protected by a thin clay cap that creates semi-confined conditions (Table 5).

Table 5. Functional borehole points and corresponding VES stations in productive areas.

Ward / Community	BH points	Status	Corresponding VES	Aquifer characteristics
Shamaki	B13, B35, B40, B47	Functional	VES 16 (Kagarawal)	Fine-grained sandstone aquifer at 70–80 m
Herwagana	B53, B56, B66	Functional	VES 8 (Kanoyel Qtrs)	Medium- to fine-grained sand aquifer at 55–65 m
Dawaki (Central)	B51, B59, B60	Functional	—	Weathered sections of lower Gombe Sandstone
Pantami (deep)	B15, B23, B27	Functional	—	Fractured zones near the Gombe Fault (> 90 m)
GRA / Lowcost	—	—	VES 13 (Fed Lowcost)	Silty sand aquifer at 90–100 m
Tumpure	—	—	VES 1 (Tumpure)	Deep sandy clay target at 150–160 m

Borehole B40 in Shamaki, reaching 128 m and yielding 10 L/s, exemplifies this pattern: VES 16 shows an aquitard of shale and mudstone between 10 and 56 m, beneath which a productive sandstone

ISSN:2584-2706 DOI: https://doi.org/10.67317/IJMSRT26AUG166

unit appears. Drilling through the initial clay/shale sequence to reach the lower Gombe sandstone is therefore a viable, ground-truthed strategy for high-yield wells in this ward.

4.5 Comprehensive VES Interpretation and Lithology–Potential Statistics

All 23 VES stations were classified by curve type, aquiferous depth, inferred lithology, and groundwater potential (Table 6). The results distinguish two productive depth tiers: a "Moderate Potential" tier (50–100 m), accessible by standard drilling and typically sufficient for community hand pumps or small motorized systems, and a "High Potential" tier (generally > 135 m) requiring deep-well technology to reach protected, high-yield aquifers likely corresponding to the basal Gombe Formation or upper Yolde Formation.

Table 6. Comprehensive VES interpretation and groundwater potential classification (all 23 stations).

VES location	Curve type	Aquiferous depth (m)	Inferred aquifer lithology	Potential
1. Tumpure Bashar	KQHA	150 – 160	Fine-grained sandy clay	High (deep)
2. Wuro Biriji	HKH	60 – 70	Fine-grained sand	Moderate
3. Hammadukafi	HKH	70 – 80	Fine-grained sand	Moderate
4. Dubai Qtrs	HKQQ	15 – 20	Fine-grained sand (thin)	Poor (dry shale below)
5. Bogo Area I	HKQ	135 – 145	Fine-grained sandstone	High (deep)
6. New Liji	HAA	40 – 50	Fine-grained sandy clay	Moderate
7. Liji	HAKH	150 – 160	Fine-grained sand	High (deep)
8. Kanoyel Qtrs	HKH	55 – 65	Fine-grained sand	Moderate
9. Doma Plaza	HAKH	135 – 145	Fine-grained sandstone	Poor (shale-capped)
10. Opp. Govt House	HKH	100 – 110	Fine-grained sand	Moderate
11. GRA Gombe	KHA	70 – 80	Silty sand	Moderate
12. New GRA	QQHK	150 – 160	Sandy silt	High (deep)
13. Fed Lowcost	HKH	90 – 100	Silty sand	Moderate
14. Dawaki Qtrs	HKH	80 – 90	Fine-grained sandstone	Moderate
15. ECWA Tudunwada	HKH	50 – 60	Fine-grained sandstone	Moderate
16. Kagarawal	HKH	70 – 80	Fine-grained sandstone	Moderate
17. Wuro Kesa	HKH	65 – 75	Fine-grained sandstone	Moderate
18. Wuro Aji	HAKH	105 – 115	Fine-grained sandstone	Moderate
19. Jauro Yaya	HAA	60 – 70	Fine-grained sand	Moderate
20. Zagaina	HKH	60 – 70	Fine-grained sand	Moderate
21. Koran Zaki	AKH	80 – 90	Fine-grained sandy silt	Moderate

ISSN:2584-2706 DOI: https://doi.org/10.67317/IJMSRT26AUG166

VES location	Curve type	Aquiferous depth (m)	Inferred aquifer lithology	Potential
22. FCE I	HKQH	140 – 150	Fine-grained sandy clay	High (deep)
23. FCE II	HAKH	150 – 160	Fine-grained sandy clay	High (deep)

Table 6b. Observed contingency table of inferred aquifer lithology by groundwater-potential class (derived from Table 6).

Lithology	Poor	Moderate	High	Total
Sand	1	6	1	8
Sandstone	1	5	1	7
Sandy clay	0	1	3	4
Sandy silt	0	1	1	2
Silty sand	0	2	0	2
Total	2	15	6	23

The lithology–potential contingency table derived from Table 6 (Table 6b) was tested using Pearson's chi-square (χ^2 (8) = 8.242, p = 0.410) and, because several expected cell frequencies were below 5, the Fisher–Freeman–Halton exact test for the 5 × 3 table (p = 0.458). The exact test does not provide evidence of a statistically significant lithology–potential association at $\alpha = 0.05$, although Cramér's V of 0.423 indicates a moderate-to-substantial descriptive association. This absence of formal significance should be interpreted cautiously given the small VES sample (n = 23) and sparse contingency table; the descriptive pattern nonetheless remains geologically meaningful. Fine-grained sandstone and clean sand aquifers account for the largest share of high-potential occurrences, while sandy clay units are predominantly moderate at shallow depth and high only where deeply confined (> 135 m). Silty sand and sandy silt lithologies are associated predominantly with moderate potential, with the New GRA station (VES 12, sandy silt, High) as a single exception; this station is flagged for verification against the original field record before submission, since the narrative synthesis elsewhere in the source dataset otherwise treats silty sand and sandy silt as consistently moderate. Poor-potential occurrences are limited and confined to thin sand bodies underlain or capped by shale (VES 4, VES 9).

ISSN:2584-2706 DOI: https://doi.org/10.67317/IJMSRT26AUG166

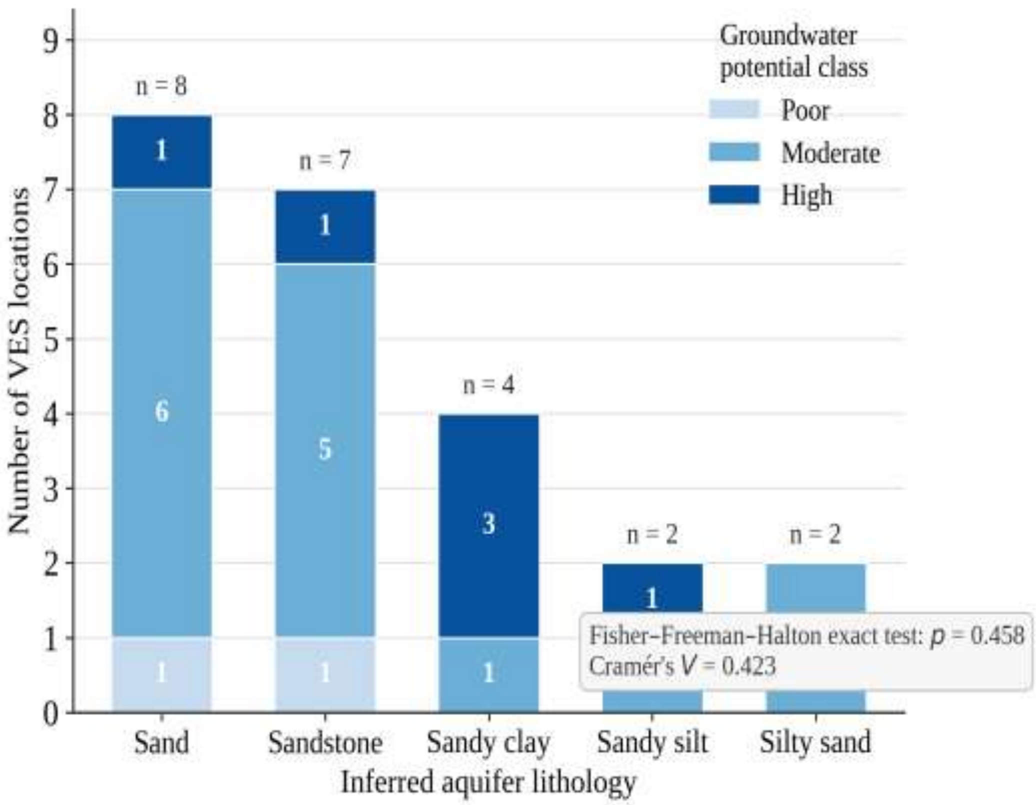

Figure 3. Lithology–groundwater-potential frequency distribution derived from Table 6. Bars show the number of VES locations per lithological class, stacked by groundwater-potential class.

4.6 Depth Control on Borehole Outcome

Figure 4 plots depth against functional status for the 24 boreholes with individually documented depth values in the compiled inventory (Table 2). Non-functional boreholes cluster between 27 and 120 m, with a visible concentration below 90 m; the documented functional boreholes span a wider and more bimodal range, from a shallow outlier at 36 m (B39) to a deep, high-yielding well at 128 m (B40), with a further functional well at an approximate 90–100 m range near Pantami (B15). This distribution is consistent with, but does not by itself statistically confirm, a depth-related control on borehole success: non-functional wells dominate the shallow-to-intermediate range, while the deepest documented well (128 m) is functional. The single shallow functional exception (B39, 36 m) and the Pantami well, whose success is attributed to fault-associated fracturing rather than depth alone (Section 5.3), demonstrate that depth is not by itself a sufficient predictor of outcome.

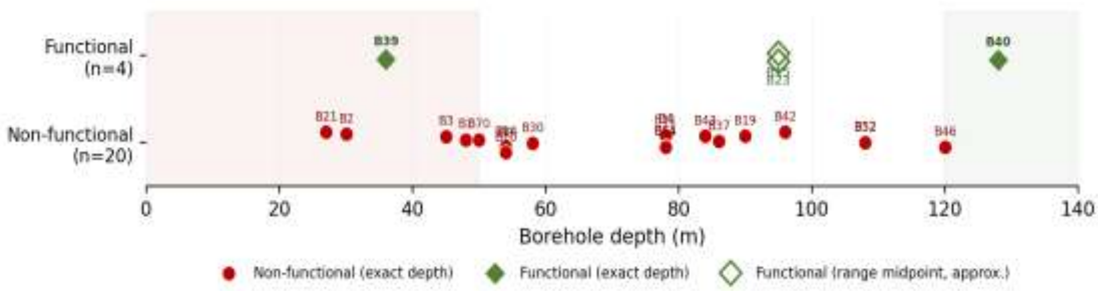

Figure 4. Depth versus functional status for the documented borehole subset (n = 24 of 71 total).

Formal statistical testing on the larger, complete-data subset (n = 58: 35 functioning, 23 not functioning) confirms this qualitative impression only partially. Functioning boreholes had a mean depth of 86.57 m (SD = 29.33, median 78.0 m, range 36–160 m); non-functioning boreholes had a mean depth of 71.96 m (SD = 30.97, median 78.0 m, range 20–145 m) (Figure 5). A two-sided Mann–Whitney U test gave U = 505.0, p = 0.105; the rank-biserial effect size was 0.255, indicating a small-

 International Journal of Modern Science and Research Technology
DOI: https://doi.org/10.67317/IJMSRT26AUG166

to-moderate tendency for functioning boreholes to be deeper, but this difference was not statistically significant at α = 0.05. This is an important, honest result: the ward-level pattern documented above (Section 4.1, 4.3, 4.4) is real and geologically interpretable, but on the full available sample, depth alone does not significantly separate functioning from non-functioning boreholes — consistent with the interpretation, developed further in Section 5, that lithological confinement and structural position, not depth in isolation, are the dominant controls.

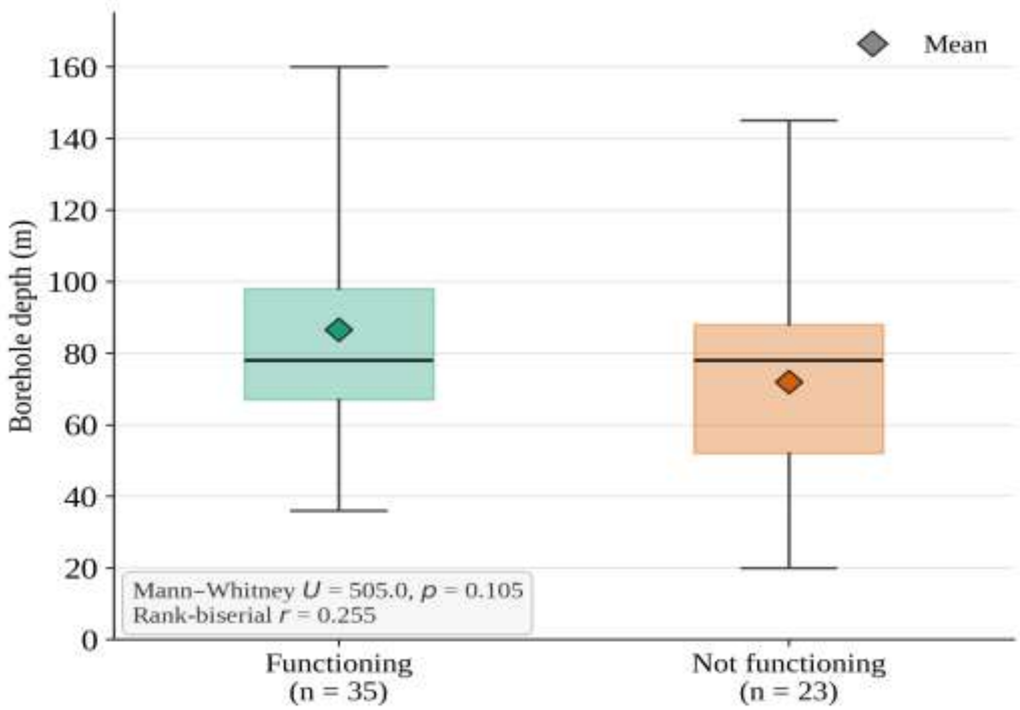

Figure 5. Borehole depth distribution by functional status (n = 58 boreholes with complete depth and status data). Boxes show the median and interquartile range; whiskers extend to the group minimum and maximum; diamonds show the group mean.

4.7 Aquiferous Depth versus Groundwater Potential

Using the midpoint of each Table 6 aquiferous-depth interval, the relationship between aquiferous depth and groundwater potential was tested directly (Figure 6). Spearman's rank correlation between depth and ordinal groundwater potential was $\rho = 0.682$, $p < 0.001$ (exact $p = 0.000336$). A Kruskal–Wallis test showed a significant difference in depth distributions among the Poor, Moderate, and High potential classes, $H(2) = 12.628$, $p = 0.002$. These results support the descriptive pattern evident in Table 6 and Figure 6: the six High-potential VES locations occur at deep aquiferous levels (≥ 135 m), Moderate locations occupy mainly intermediate depths, and the two Poor locations occur at approximately 17.5 m and 140 m. The deep Poor case (Doma Plaza, VES 9) demonstrates that depth alone is not sufficient to predict groundwater potential; lithological confinement and shale capping remain important controls, exactly as the qualitative ground-truthing in Sections 4.3–4.4 independently indicated.

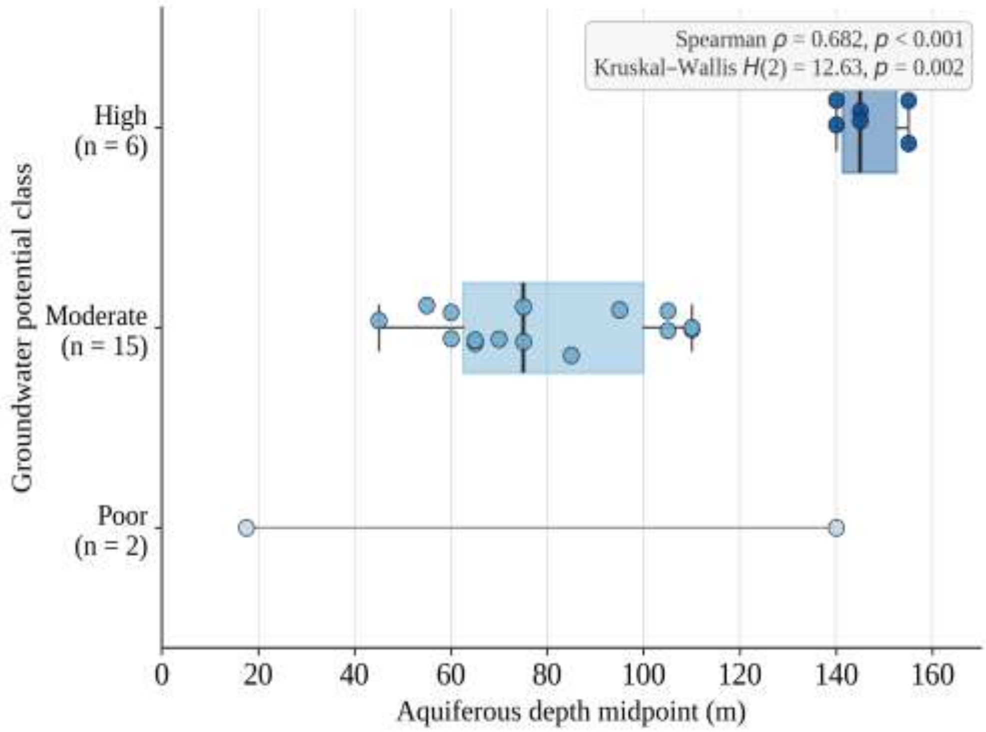

Figure 6. Aquiferous depth midpoint versus groundwater-potential class. Points show individual VES locations; boxes are shown only for classes with n ≥ 5 (Moderate, High), since quartiles are not meaningfully defined at n = 2 (Poor).

4.8 Consolidated Statistical Summary

Table 7 consolidates the statistical tests applied across the borehole and VES datasets.

Table 7. Summary of statistical tests applied to the borehole and VES datasets.

Relationship examined	Test applied	Statistic	p-value	Effect size
Lithology × groundwater potential	Pearson chi-square	$\chi^2(8) = 8.242$	0.410	Cramér's V = 0.423
Lithology × groundwater potential	Fisher–Freeman–Halton exact	—	0.458	—
Borehole depth × functional status (n=58)	Mann–Whitney U	U = 505.0	0.105	r = 0.255
Aquiferous depth × groundwater potential	Spearman rank correlation	$\rho = 0.682$	< 0.001	—
Aquiferous depth × groundwater potential	Kruskal–Wallis H	H(2) = 12.628	0.002	—

ISSN:2584-2706 DOI: https://doi.org/10.67317/IJMSRT26AUG166

5. Discussion

5.1 The Shale Trap and Ironstone Capping as Dominant Failure Mechanisms

The most frequent cause of failure in Bolari and Jakada Fari is the Pindiga (Fika) Shale, which acts as an aquiclude; boreholes terminating within its 15–110 m depth range are consistently dry (Section 4.3). A related but mechanistically distinct failure mode occurs in Bolari East and Kumbiya-Kumbiya, where high-resistivity ironstone and mudstone layers (VES 4 and VES 12) can be, and evidently were, mistaken for a "basement" or "dry sand" signature by drillers, leading to premature abandonment of wells such as B9 and B46. This distinction matters operationally: a shale-terminated well requires deeper drilling through a genuine aquiclude, whereas an ironstone-terminated well may in fact overlie a thin saturated sand horizon masked by the resistivity contrast of the ironstone cap. Only comparison against functional-well logs such as B40 or B56 allows this ambiguity to be resolved, which is precisely the ground-truthing logic this study formalizes.

5.2 Structural Attenuation and the Limits of a Purely Stratigraphic Model

Near the Gombe Fault, sedimentation cycles produce fine-grained, thinly bedded, "flysch-like" sequences with insufficient thickness for water accumulation, rendering the Gombe Formation locally non-aquiferous despite its considerable thickness elsewhere in the metropolis. This confirms that a purely stratigraphic model of aquifer occurrence, based on formation identity alone, is inadequate in Gombe: the same formation can be highly productive in one ward and structurally compromised in another, depending on proximity to the fault and the resulting facies attenuation.

5.3 Structural Interference as a Positive Control: The Pantami Exception

At Pantami, functional wells at 90–100 m (B15, B23) contradict the general trend of shallow failure observed in nearby Bolari. The most defensible geological interpretation is that the Gombe Fault has generated localized fractured zones that act as conduits for groundwater flow. In the absence of borehole evidence, a geophysical interpretation alone might well have dismissed Pantami as unproductive, given the substantial shale content evident in outcrop. Adherence to borehole success records in this ward instead permits a targeted geophysical search for these fracture zones elsewhere along the fault trend, which is among the more actionable recommendations of this study (Section 6).

5.4 Depth as a Statistically Partial, Lithology-Conditioned Predictor

The statistical results in Section 4.6 and 4.7 sharpen, rather than contradict, this picture. Aquiferous depth is strongly and significantly associated with VES-derived groundwater potential ($\rho = 0.682$, $p < 0.001$), confirming quantitatively what the ward-level ground-truthing suggested descriptively: deeper interpreted aquifer units are systematically more productive. Borehole depth alone, however, does not significantly distinguish functioning from non-functioning boreholes on the full 58-record subset ($U = 505.0$, $p = 0.105$). Read together, these two results indicate that depth matters chiefly as a proxy for reaching a favorable lithological unit — typically below the shale and ironstone barriers described in Sections 5.1–5.2 — rather than as an independent driver of success. The shallow B39 exception and the fault-controlled Pantami wells illustrate the same point from the qualitative side: lithological connectivity and structural context can override a simple depth rule in either direction. Practically, this means depth-based drilling guidance (Section 6) should be read as a probabilistic, lithology-conditioned heuristic rather than as a deterministic threshold applicable without regard to structural and stratigraphic position.

5.5 Toward Multivariate and Spatial Models

The formal statistical testing undertaken in this study (Section 3.5, Section 4.6–4.8) substantially addresses the quantitative threshold analysis identified as a priority in earlier drafts of this work, confirming a significant depth–potential relationship for aquiferous depth while showing that borehole depth alone is not a significant predictor of functional status on current data. Two further analyses would still strengthen the evidentiary basis for groundwater development planning in Gombe: a multivariate model (e.g. logistic regression) of borehole success as a joint function of depth, ward, and nearest-VES potential class, fitted to the complete 71-borehole register once fully digitized, since the present Mann–Whitney comparison necessarily considers depth alone; and a cost-benefit analysis of drilling depth that weighs incremental drilling cost against probability of success, which preliminary reasoning suggests may favor intermediate rather than maximal depths at specific sites once actual unit drilling costs are obtained. We identify these as priority directions for follow-up analysis rather than reporting them as completed findings, since the underlying cost data and the remaining uncompiled borehole records were not available within the scope of the present dataset.

5.6 Groundwater Quality and Public Health Considerations

Sustainability of a water source is defined by quality as well as yield. The Gombe Sandstone is a documented source of iron-laden water, with leaching of terrestrial salts and oxidation of ironstone beds elevating dissolved iron and phosphate concentrations, particularly at Pantami and parts of Jakada Fari; while these concentrations may not always exceed World Health Organization toxicity thresholds, they render water aesthetically undesirable for laundry and cooking, pushing residents toward costly alternatives such as water tankers. Dense urbanization in central wards, combined with the poor-to-weak protective capacity indicated by longitudinal conductance in several VES stations, is consistent with elevated contamination risk from pit latrines and surface runoff, a concern corroborated by prior local water-quality work (Sabo, 2012). We note, however, that the bacteriological findings referenced in the underlying dataset originate from a separate study and are cited here for context rather than presented as an original result of the present hydrogeophysical assessment; any bacteriological or hydrochemical claims retained in the final submission should be supported by an explicit sampling and laboratory methodology or clearly attributed to the cited source.

6. Conclusions and Recommendations

This study integrated 71 borehole records and 23 Vertical Electrical Sounding stations, tested with formal non-parametric statistics, to assess the causes of borehole failure and the distribution of groundwater potential in Gombe Metropolis, northeastern Nigeria — a setting broadly representative of groundwater development challenges across the Global South. The hydrogeological landscape of the metropolis is defined by pronounced heterogeneity, and success in groundwater development is shown to depend not on chance but on the joint influence of aquiferous depth and lithological confinement: aquiferous depth is strongly and significantly associated with VES-derived groundwater potential ($\rho = 0.682$, $p < 0.001$), while borehole depth alone does not significantly distinguish functioning from non-functioning boreholes ($p = 0.105$), underscoring that lithology and structure, not depth in isolation, govern outcome.

The most productive wells bypass the dry shale members of the Pindiga Formation and the middle Gombe member to tap either the lower Gombe Formation (70–120 m) or the deeper Yolde Formation (> 180 m); HKH and HAKH curve types are the most reliable geoelectric indicators of these conditions. Failure is concentrated in Bolari and Jakada Fari, where thick Pindiga Shale and ironstone intercalations act as barriers, and shallow termination (30–50 m) in these wards leads to near-certain failure. Throughout, geophysical interpretation is shown to require constraint by borehole ground-truth: the high resistivity of ironstone can easily be mistaken for an aquiferous sand layer, and only comparison against the logs of confirmed functional wells, combined with the statistical evidence in Section 4, resolves this ambiguity.

7. Recommendations

1. Deep-well priority, lithology-conditioned: for municipal-scale reliability, drilling should transition toward deeper boreholes (180–300 m) targeting the Yolde and Bima Formations where feasible, but depth targets should always be read against the nearest VES lithological interpretation (Table 6) rather than applied as a uniform rule, since depth alone was not a statistically significant predictor of success in this dataset.

2. Geophysical protocol: future VES surveys should employ larger current electrode spreads (AB/2 > 200 m) to image deep targets reliably and avoid misinterpretation caused by shallow ironstone capping.
3. Ward-specific planning: development in Pantami should prioritize structural mapping to locate fault-induced fracture zones, while development in Shamaki should focus on penetrating the middle-member aquitard to reach the productive lower-member sandstone.
4. Health and quality integration: every new borehole should include iron and bacteriological testing as standard practice, with on-site treatment considered in densely built-up central wards.
5. Data infrastructure: the ward, state, or federal agency responsible for borehole records should digitize and centralize the complete 71-borehole inventory, including coordinates and yield, to enable the multivariate and spatial models proposed in Section 5.5 and to support routine, evidence-based siting decisions beyond the scope of any single study.

Declarations
Conflict of interest: The authors declare no conflicts of interest
Data availability: Data to be make available on reasonable request
Funding: *This research work receives no funding statement*

References
1. Adelana, S. M., & MacDonald, A. M. (2008). Groundwater research issues in Africa. Applied groundwater studies in Africa, 1-8.
2. Ajayi, O. G., Nwadialor, I. J., Odumosu, J. O., Adetunji, O. O., & Abdulwasiu, I. O. (2022). Assessment and delineation of groundwater potential zones using integrated geospatial techniques and analytic hierarchy process. *Applied Water Science*, *12*(12), 276.
3. Ascott, M. J., Macdonald, D. M. J., Sandwidi, W. J. P., Black, E., Verhoef, A., Zongo, G., ... & Cook, P. (2022). Time of emergence of impacts of climate change on groundwater levels in sub-Saharan Africa. Journal of Hydrology, 612, 128107.
4. Babaye, M. S. A., Hantchi, K. D., Wagani, I., Ousmane, B. I., & Sandao, I. (2021). Multi-criteria analysis using remote sensing and GIS: insight into groundwater potential of the fissured aquifers in the Liptako socle (southwestern Niger).
5. Cobbing, J., & Hiller, B. (2019). Waking a sleeping giant: Realizing the potential of groundwater in Sub-Saharan Africa. World Development, 122, 597-613.
6. Coomar, P., & Mukherjee, A. (2020). Global geogenic groundwater pollution. 187-213. https://doi.org/10.1016/b978-0-12-818172-0.00014-1
7. Cuthbert, M. (2026). What is groundwater? *Hydrogeology Journal*. https://doi.org/10.3133/ofr93643
8. Cuthbert, M. O., Gleeson, T., Moosdorf, N., Befus, K. M., Schneider, A., Hartmann, J., & Lehner, B. (2019). Global patterns and dynamics of climate–groundwater interactions. Nature Climate Change, 9(2), 137-141.
9. Cuthbert, M. O., Taylor, R. G., Favreau, G., Todd, M. C., Shamsudduha, M., Villholth, K. G., ... & Kukuric, N. (2019). Observed controls on resilience of groundwater to climate variability in sub-Saharan Africa. *Nature*, *572*(7768), 230-234.
10. Danert, K., Adekile, D., & Canuto, J. G. (2020). Striving for borehole drilling professionalism in Africa: a review of a 16-year initiative through the rural water supply network from 2004 to 2020. Water, 12(12), 3305.
11. Danert, K., Adekile, D., Malik, M., Museteka, L., & Abuuru, D. (2022). Achievements and lessons learned in the implementation of groundwater regulation in Zambia. Water Resources Management Authority, Lusaka. https://www. rural-water-supply. net/en/resources/details/1040 [accessed 28 February 2022].
12. Egbueri, J. C., Agbasi, J. C., Onuba, L. N., Nweke, N. D., Uwajingba, H. C., & Abba, S. I. (2025). Groundwater development within the Nigerian crystalline and sedimentary aquifers: challenges and opportunities. Groundwater in developing countries: Case studies from MENA, Asia and West Africa, 297-325.
13. Foster, S., & MacDonald, A. (2014). The ‘water security’dialogue: why it needs to be better informed about groundwater. *Hydrogeology Journal*, *22*(7), 1489-1492.

ISSN:2584-2706 DOI: https://doi.org/10.67317/IJMSRT26AUG166

14. Garba, M. A., Zubairu, C. S., & Garba, M. A. (2025). Multivariate Hydrochemical Characterization and Spatial Variability of Groundwater Quality in Kano Region, Nigeria: Insights into Natural Geology and Anthropogenic Influence. DOI: https://doi. org/10.20944/preprints202508, 2043, v1.
15. Hansani, U., Witharana, S. A., Dharmapriya, P. L., Wijekoon, P., Wu, Z., Chen, X., ... & Weerasooriya, R. (2025). Multivariate Analysis and Hydrogeochemical Evolution of Groundwater in a Geologically Controlled Aquifer System: A Case Study in North Central Province, Sri Lanka. Water, 18(1), 89.
16. Jimoh, J. B., Musa, O. K., & Ahmed, I. I. (2025). AN INTEGRATED METHOD FOR MAPPING GROUNDWATER POTENTIAL IN PART OF ABUJA, CENTRAL NIGERIA. *Scientia Africana*, *24*(1), 339-362.
17. Mukherjee, A. (2018). Overview of the Groundwater of South Asia. 3-20. https://doi.org/10.1007/978-981-10-3889-1_1
18. Osinowo, O. O., & Arowoogun, K. I. (2020). A multi-criteria decision analysis for groundwater potential evaluation in parts of Ibadan, southwestern Nigeria. *Applied Water Science*, *10*(11), 228.
19. Xu, Y., & Braune, E. (2010). Sustainable groundwater resources in Africa. *Water supply and sanitation environment*, 23.